

## Research Article

# Dynamic Decoupling Control Optimization for a Small-Scale Unmanned Helicopter

Rui Ma <sup>1</sup>, Li Ding <sup>2</sup>, and Hongtao Wu<sup>1</sup>

<sup>1</sup>College of Mechanical and Electrical Engineering, Nanjing University of Aeronautics and Astronautics, Nanjing 210016, China

<sup>2</sup>College of Mechanical Engineering, Jiangsu University of Technology, Changzhou 213001, China

Correspondence should be addressed to Li Ding; [nuaadli@163.com](mailto:nuaadli@163.com)

Received 22 January 2018; Revised 27 March 2018; Accepted 22 April 2018; Published 27 June 2018

Academic Editor: Huosheng Hu

Copyright © 2018 Rui Ma et al. This is an open access article distributed under the Creative Commons Attribution License, which permits unrestricted use, distribution, and reproduction in any medium, provided the original work is properly cited.

This article presents design and optimization results from an implementation of a novel disturbance decoupling control strategy for a small-scale unmanned helicopter. Such a strategy is based on the active disturbance rejection control (ADRC) method. It offers an appealing alternative to existing control approaches for helicopters by combining decoupling and disturbance rejection without a detailed plant dynamics. The tuning of the control system is formulated as a function optimization problem to capture various design considerations. In comparison with several different iterative search algorithms, an artificial bee colony (ABC) algorithm is selected to obtain the optimal control parameters. For a fair comparison of control performance, a well-designed LQG controller is also optimized by the proposed method. Comparison results from an attitude tracking simulation against wind disturbance show the significant advantages of the proposed optimization control for this control application.

## 1. Introduction

In recent years, rotary-wing Unmanned Aerial Vehicles (UAVs) including quadrotors, helicopters, and ducted fans are attractive to industries and academia [1, 2]. With the unique features such as hovering, good maneuverability, and low costs, they have been applied to diverse domains by installing different sensors, cameras, or other payloads on the platform [3, 4]. However, due to the complexity of flight dynamics, it is still challenging to design an appropriate flight control system that satisfies the requirement for autonomous flight.

Small-scale unmanned helicopter is a representative of the rotary-wing UAVs. It is considered as an inherently unstable, highly nonlinear, and underactuated system with significant dynamic coupling. With the small size and agile maneuverability, it is more susceptible to gust disturbance than those full-sized counterpart. Furthermore, the dynamic parameters change with the load and flight conditions. These factors cause serious challenges in dealing with concerns about the robustness, disturbance rejection, decoupling, and other control problems. To address the above problems, the classical single-input/single-output (SISO) feedback control

methods are implemented in [5–7]. In these researches, the controller is optimized based on the identified model established firstly for a small helicopter. Nevertheless, many researchers have recognized that the complexity nature of helicopter and better control capability requires more advanced technologies. Cases include direct adaptive neural command controller [8], adaptive control methods [9], nonlinear control methods [10], vision-based guidance control techniques [11], and intelligent control methods like fuzzy logic approach [12] and neural network [13]. And the most pervasive choice in practical applications is the robust control approach: for example, the Kalman filter-based linear quadratic integral (LQI) approach [14], linear quadratic regulator (LQR) [15], and the  $H_\infty$  control approach [16, 17]. These methods provide a reasonable countermeasure for both disturbances and multivariable effects of the helicopter. However, the effectiveness of the prevailing model-based control approaches is exceedingly dependent on the exact model and aerodynamic coefficients of the plant. Facing the complicated control problem of the helicopter, the effective solution is to compensate the disturbance immediately and reduce the dependence of plant model.

TABLE 1: Physical descriptions of the state and input variables of the helicopter dynamical model.

Variable	Physical significance	Unit
$P = [X, Y, Z]^T$	Position in Earth-fixed coordinate frame	m
$V = [u, v, w]^T$	Velocity vector along body frame X-, Y-, and Z-axes	m/s
$\Omega = [p, q, r]^T$	Roll, pitch, and yaw angular rates	rad/s
$\Theta = [\varphi, \theta, \psi]^T$	Euler angles	rad
$a_s, b_s$	Longitudinal and lateral main rotor flapping angle	rad
$r_{fb}$	Intermediate state in yaw rate feedback controller dynamics	N/A
$u_{lat}$	lateral cyclic rotor control input	N/A
$u_{lon}$	longitudinal cyclic rotor control input	N/A
$u_{col}$	collective pitch control input	N/A
$u_{ped}$	tail rotor pedal control input	N/A

The main contribution of this paper is introducing a dynamic decoupling control (DDC) strategy [18] and its optimization method to a small-scale helicopter. This strategy is rooted in active disturbance rejection control (ADRC) that was recently proposed by Han [19]. The key idea of the method is to treat the total disturbance (incorporating the interactions among control loops and the unknown external disturbances) as a state variable, which can be estimated by an extended state observer (ESO) through the input-output data of the plant in real time. Consequently, unlike most existing model-dependent control methods, very little information of the model is required for ADRC [20]. ADRC offers a practical solution to decoupling control problems in the presence of large uncertainties and has been successfully applied in many engineering applications, e.g., aircraft flight control [21] and the chemical processes [22]. Moreover, in order to simplify the implementation of ADRC, Gao proposed the linear active disturbance rejection control (LADRC), which offers much better performance and needs few parameters to tune, and detailed comparison studies can be found in [23].

Since the performance of LADRC depends on the convergence speed of state observer, the bandwidth of which is the most important tuning parameter. Obviously, the trade-offs between the robustness and performance have always been difficult, especially for the helicopter. This problem can be solved by using a multiobjective optimization algorithm in the simulated environment. Artificial bee colony algorithm (ABC) was first proposed by Karaboga in 2005 [24] and successfully applied to control optimization, including optimal tuning of PID controller in [25], optimized LQR controller in [26], and robust fuzzy PSS design [27]. As we have known, usual optimization algorithms conduct only one search operation in one iteration, but ABC algorithm can conduct both local search and global search in each iteration; as a result, the probability of finding the optimal parameters is significantly increased, which efficiently avoids local optimum to a large extent.

This paper considers a design and optimization of the DDC controller used in our TREX-600 helicopter. As a controlled plant, the dynamical model is obtained through the system identification method in previous work [26]. The main idea can be characterized as follows: (i) in the design of decoupling control, all the information needed is only the

predetermined input-output pairing of helicopter's dynamic model, (ii) the effect of one input to all other outputs that is not paired with, namely, the cross channel interference is viewed as a 'disturbance' to be actively estimated and canceled out in DDC framework, and (iii) the parameter tuning problem is transformed into a functional optimization problem defined by a combination of different control performance indexes, and ABC algorithm is introduced to calculate the optimal solution. Using this approach, we can optimize controllers with different control requirement.

The paper is organized as follows. In Section 2, the helicopter dynamical model under consideration is briefly introduced. Section 3 describes how to use DDC strategy to decouple the helicopter. Section 4 formulates the parameter optimization problem. Simulation tests on the model are shown in Section 5. Finally, the main conclusions are summarized in Section 6.

## 2. System Model for Unmanned Small-Scale Helicopter

Based on the first principle approach, the dynamics of helicopter is regarded as a six-degrees-of-freedom rigid-body dynamics augmented with a simplified main rotor flapping dynamics and a factory-installed yaw rate gyro dynamics. As illustrated in Figure 1 and summarized in Table 1, this model contains fifteen states and four inputs. Detailed information of the physical parameters and modeling structure can be found in [28]. A brief overview of the flight dynamical model is presented next.

The translational motion and rotational motion of the helicopter [15] are described as

$$\begin{aligned}
 \dot{P} &= R(\Theta) V, \\
 \dot{\Theta} &= S(\Theta) \Omega, \\
 \dot{V} &= \frac{\mathbf{F}_b}{m} + \frac{\mathbf{F}_g}{m} - \Omega \times V \\
 \dot{\Omega} &= \mathbf{I}^{-1} [\mathbf{M}_b - \Omega \times (\mathbf{I}\Omega)]
 \end{aligned} \tag{1}$$

where  $\mathbf{F}_g = [-mg \sin \theta, mg \sin \phi \cos \theta, mg \cos \theta \cos \phi]^T$  is the gravity force vector projected onto the body frame (BF);  $m$

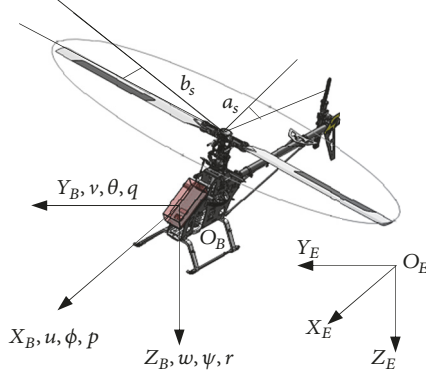


FIGURE 1: Illustration for helicopter states and coordinates.

is the helicopter mass;  $\mathbf{I} = \text{diag}\{I_{XX}, I_{YY}, I_{ZZ}\}$  is the inertial moment matrix about the reference axes;  $\mathbf{F}_b$  and  $\mathbf{M}_b$  denote the combined aerodynamic force and moment vectors acting on the helicopter center of gravity (CG), respectively. The transformation matrices  $R$  and  $S$  are, respectively, given as

$$R = \begin{bmatrix} c_\theta c_\psi & s_\phi s_\theta c_\psi - c_\phi s_\psi & c_\phi s_\theta c_\psi + s_\phi s_\psi \\ c_\theta s_\psi & s_\phi s_\theta s_\psi + c_\phi c_\psi & c_\phi s_\theta s_\psi + s_\phi c_\psi \\ -s_\theta & s_\phi c_\theta & c_\phi c_\theta \end{bmatrix}, \quad (2)$$

$$S = \begin{bmatrix} 1 & t_\theta s_\phi & t_\theta c_\phi \\ 0 & c_\phi & -s_\phi \\ 0 & \frac{s_\phi}{c_\theta} & \frac{c_\phi}{c_\theta} \end{bmatrix}, \quad (3)$$

in which the compact notations  $s_{(*)}$ ,  $c_{(*)}$ , and  $t_{(*)}$  denote  $\sin(*)$ ,  $\cos(*)$ , and  $\tan(*)$ , respectively.

In the helicopter system,  $\mathbf{F}_b$  and  $\mathbf{M}_b$  are generated by the aerodynamic forces of the fuselage and the control forces which originate from the main rotor thrust and tail rotor thrust. Generally, we calculate  $\mathbf{F}_b$  and  $\mathbf{M}_b$  without the consideration of the aerodynamic forces of fuselage due to the relatively small influence on the model. Therefore, the force and moment components in the BF are, respectively, given by

$$\mathbf{F}_b = \begin{bmatrix} F_X \\ F_Y \\ F_Z \end{bmatrix} = \begin{bmatrix} -T_{mr} \sin a_s \\ T_{mr} \sin b_s - T_{tr} \\ -T_{mr} \cos a_s \cos b_s \end{bmatrix}, \quad (4)$$

$$\mathbf{M}_b = \begin{bmatrix} L \\ M \\ N \end{bmatrix} = \begin{bmatrix} (K_\beta + T_{mr} H_{mr}) \sin b_s - T_{tr} H_{tr} \\ (K_\beta + T_{mr} H_{mr}) \sin a_s \\ N_{mr} + T_{tr} D_{tr} \end{bmatrix} \quad (5)$$

where  $T_{mr}$ ,  $N_{mr}$ , and  $T_{tr}$  are the main rotor thrust and moment and the tail rotor thrust, respectively;  $D_{tr}$  is the distance from the CG to the tail rotor hub, along the  $x$  direction;  $H_{mr}$  and  $H_{tr}$  are the distance from the CG to the main rotor and tail rotor hub, along the  $z$  direction, respectively, and  $K_\beta$  is the main rotor spring constant.

The main rotor flapping dynamics, which are common to all small-scale helicopters, is described by the following two coupled first-order differential equations [29]:

$$\begin{bmatrix} \dot{a}_s \\ \dot{b}_s \end{bmatrix} = \begin{bmatrix} -q - \frac{a_s}{\tau_f} + A_b b + A_{lon} u_{lon} \\ -p + B_a a_s - \frac{b_s}{\tau_f} + B_{lat} u_{lat} \end{bmatrix} \quad (6)$$

where  $\tau_f$  is the main rotor time constant;  $A_b$  and  $B_a$  are cross coupling derivatives that influence the longitudinal and lateral flapping motions; and  $A_{lon}$  and  $B_{lat}$  are effective linkage gains.

Since the high sensitivity of the bare yaw channel dynamics, a feedback yaw rate controller is widely used in small-scale helicopters. The UAV system reserved this feature for the convenience of manual control. Accordingly, the augmented yaw dynamics are modeled as a first-order bare airframe dynamics with a yaw rate feedback represented by a simple first-order low-pass filter [30]. The corresponding differential equations are given as

$$\begin{bmatrix} \dot{r} \\ \dot{r}_{fb} \end{bmatrix} = \begin{bmatrix} N_r r + N_{ped} (u_{ped} - r_{fb}) \\ -K_{rfb} r_{fb} + K_r r \end{bmatrix} \quad (7)$$

where  $N_r$ ,  $N_{ped}$ ,  $K_r$ , and  $K_{rfb}$  are the parameters to be identified.

### 3. Dynamic Decoupling Control (DDC) of the Helicopter

**3.1. LESO Based Dynamic Decoupling Control Method.** Linear Active Disturbance Rejection Controller (LADRC) is a novel control method which is parameterized from ADRC [20] to simplify the tuning process. In this work, LADRC-based DDC approach [18] is implemented to tackle the decoupling problem for helicopter attitude dynamics. Define  $f_i$  as the combined effect of the internal coupling dynamics and external disturbances in each channel:

$$f_i = h_i(x, x^{(1)}, \dots, x^{(n_i-1)}, w_i) + \sum_{j=1}^m b_{ij} u_j - b_{ii} u_i \quad (8)$$

Then, the helicopter model can be seen as a set of coupled input-output equations with a predetermined relationship:

$$\begin{aligned} y_1^{(n_1)} &= f_1 + b_{11} u_1 \\ &\vdots \\ y_i^{(n_i)} &= f_i + b_{ii} u_i \\ &\vdots \\ y_m^{(n_m)} &= f_m + b_{mm} u_m \end{aligned} \quad (9)$$

where  $w_i$  and  $x$  are external disturbances and state vector, respectively;  $u_i$  and  $y_i$  are the dominant input and output of the  $i^{\text{th}}$  loop ( $i = 1, 2, \dots, m$ ), respectively;  $b_{ij}$  is the input gain; superscript ( $n_i$ ) denotes the  $n_i$   $\text{th}$  order derivative. Assuming the order  $n_i$  are given, the numbers of inputs and outputs are the same.

Most existing decoupling control approaches assume the knowledge of the elaborate plant model or disturbance model, which is a considerable challenge in practice. LADRC makes a breakthrough that realistically estimates  $f_i$  in real time from input-output data instead of identifying an accurate mathematical model. The idea is introduced next.

Define an enlarged state vector  $\bar{x}_i = (y_i, \dot{y}_i, \dots, y_i^{(j-1)}, f_i)$ ,  $j = 1, 2, \dots, n_i$ , in which  $f_i$  is added as an extended state. Assume  $f_i$  is differentiable and  $v_i = \dot{f}_i$  is bounded. Then the augmented state-space form of  $i^{\text{th}}$  loop in (9) is represented as

$$\begin{aligned} \dot{\bar{x}}_i &= \mathbf{A}\bar{x}_i + \mathbf{B}u_i + \mathbf{G}v_i \\ \mathbf{y} &= \mathbf{C}\bar{x}_i \end{aligned} \quad (10)$$

where

$$\begin{aligned} \mathbf{A} &= \begin{bmatrix} 0 & 1 & 0 & \cdots & 0 \\ 0 & 0 & 1 & \cdots & 0 \\ \vdots & \vdots & \vdots & \ddots & \vdots \\ 0 & 0 & 0 & \cdots & 1 \\ 0 & 0 & 0 & \cdots & 0 \end{bmatrix}, \\ \mathbf{B} &= \begin{bmatrix} 0 \\ 0 \\ \vdots \\ b_{0,i} \\ 0 \end{bmatrix}, \\ \mathbf{G} &= \begin{bmatrix} 0 \\ 0 \\ \vdots \\ 0 \\ 1 \end{bmatrix}, \\ \mathbf{C} &= \begin{bmatrix} 1 \\ 0 \\ \vdots \\ 0 \\ 0 \end{bmatrix}^T. \end{aligned} \quad (11)$$

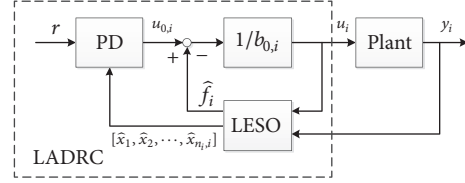


FIGURE 2: The block diagram of LADRC.

Based on the state-space model, a linear extended state observer (LESO) is designed to estimate  $\bar{x}_i$ :

$$\begin{aligned} \dot{\hat{x}}_i &= \mathbf{A}\hat{x}_i + \mathbf{B}u_i + \mathbf{L}_i(y_i - \hat{y}_i) \\ \hat{y}_i &= \hat{x}_i \end{aligned} \quad (12)$$

where  $\mathbf{L}_i = [l_{1,i}, l_{2,i}, \dots, l_{n_i+1,i}]^T$  is the observer gain needed to be chosen.

With a properly selected observer gain, the system states and  $f_i$  will be accurately estimated by the LESO in real time. The following control law for  $i^{\text{th}}$  loop can be designed to reduce the closed-loop system approximately to a unit gain cascaded integrator plant  $y_i^{(n_i)} = f_i + b_{ii}u_i \approx u_{0,i}$ :

$$u_i = \frac{u_{0,i} - \hat{f}_i}{b_{i,i}} \quad (13)$$

It is a relatively simple control problem, which is solved by using a PD controller with a feedforward term:

$$u_{i,0} = k_{1,i}(r_i - \hat{x}_{1,i}) + \cdots + k_{n_i,i}(r_i^{(n_i-1)} - \hat{x}_{n_i,i}) + r_i^{(n_i)} \quad (14)$$

where  $(k_{1,i}, k_{2,i}, \dots, k_{n_i,i})$  are the controller gains to be selected and  $r_i$  is the trajectory reference. The structure of LADRC is shown in Figure 2.

**3.2. Parameterization of LADRC.** For simplicity and practicality, both of the LESO and PD controller are parameterized in a special case as suggested in [18], where all the observer poles and controller poles are placed at  $-\omega_{0,i}$  and  $-\omega_{c,i}$ , respectively. The characteristic polynomials of (12) and (14) are constituted, respectively, as

$$\lambda_{o,i}(s) = s^{n_i+1} + l_{1,i}s^{n_i} + \cdots + l_{n_i+1,i} = (s + \omega_{0,i})^{n_i+1} \quad (15)$$

$$\lambda_{c,i}(s) = s^{n_i} + k_{n_i,i}s^{n_i-1} + \cdots + k_{1,i} = (s + \omega_{c,i})^{n_i} \quad (16)$$

with

$$l_{j,i} = \frac{(n_i + 1)! \omega_{0,i}^j}{j! (n_i + 1 - j)!}, \quad j = 1, 2, \dots, n_i + 1 \quad (17)$$

$$k_{j,i} = \frac{n_i! \omega_{c,i}^{n_i-j+1}}{(j-1)! (n_i - j + 1)!}, \quad j = 1, 2, \dots, n_i \quad (18)$$

It makes  $\omega_{0,i}$ ,  $\omega_{c,i}$  the bandwidth and the only tuning parameters for LESO and the PD controller, respectively. In

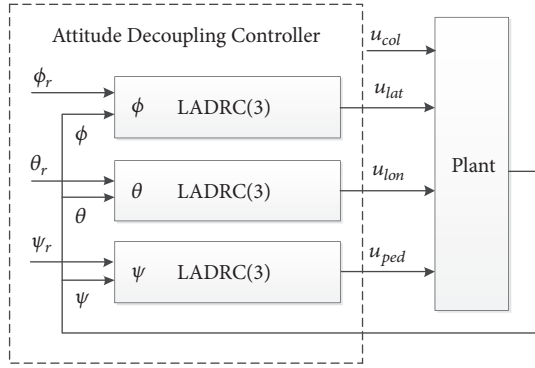


FIGURE 3: The block diagram of the attitude decoupling controller.

general, higher bandwidth corresponds to better transient response, disturbance estimation, and rejection. However, too large a value of  $\omega_{0,i}$  would cause oscillation in states. The measurement noise and excessive increase of  $\omega_{c,i}$  make the control signal oversize in magnitude and change rate. On the other hand, an appropriate selection of  $\omega_{0,i}$  and  $\omega_{c,i}$  should be subjected to physical limits and dynamic characteristics of the plant.

As seen above, the LADRC approach is a practical method for decoupling control of MIMO system. The satisfied performance will be obtained by tuning only two parameters  $\omega_{0,i}$  and  $\omega_{c,i}$ . Furthermore, it works without the detail model of the original plant, except the orders of each input-output pairs and input gains  $b_{ii}$ . The proofs of stability are given in [31, 32].

**3.3. Attitude Controller Design for the Helicopter.** As shown in Figure 3, the decoupling controller is designed to have the form of three LADRC controllers. Moreover, we selected their orders according to the relative degrees of the dynamical model. It is assumed that the controlled output  $\Theta = [\varphi, \theta, \psi]^T$  can be measured directly and that the trim value  $r = [\varphi_r, \theta_r, \psi_r]^T$  is within the physical limitation of helicopter flight.

To use the DDC approach, the order of input-output pairs in the model must be explicit. Figure 4 displays the interconnection of the helicopter subsystems, which offers a more physically meaningful design. Note that the helicopter attitude dynamics can be separated in two interconnected subsystems [6], i.e., the lateral and longitudinal subsystem and yaw dynamics. The cyclic commands  $u_{lon}$  and  $u_{lat}$  control the pitch and roll moment, and the pedal command  $u_{ped}$  manipulates the heading of the helicopter. In this case, we set the lateral and longitudinal subsystem as two third-order systems and the yaw dynamics as a second-order system.

According to aforementioned discussion and analysis, we define  $f_1$ ,  $f_2$ , and  $f_3$  as the total disturbance in each channel and rewrite (9) as

$$\begin{aligned} \phi^{(n_1)} &= f_1 + b_{01}u_{lat} \\ \theta^{(n_2)} &= f_2 + b_{02}u_{lon} \\ \psi^{(n_3)} &= f_3 + b_{03}u_{ped} \end{aligned} \quad (19)$$

where  $b_{01}$ ,  $b_{02}$ , and  $b_{03}$  are the input gains of lateral cyclic, longitudinal cyclic, and tail rotor collective pitch, respectively. In the LADRC design, these input gains are treating as another tuning parameter besides  $\omega_{0,i}$  and  $\omega_{c,i}$  to improve the performance of the reduced order closed-loop system. Note that the orders of each loop are  $n_1 = n_2 = 3$  and  $n_3 = 2$ , and the LADRC-based DDC controller can be realized by designing the LESO and PD controller for each loop, accordingly.

## 4. Optimization Problem Formulation

**4.1. The Objective Function.** The proposed LADRC tuning method using ABC is schematically shown in Figure 5, where the plant is the identified model of the TREX-600 helicopter. As stated above, the primary concern in the implementation of LADRC is maximizing the bandwidth  $\omega_{0,i}$  and  $\omega_{c,i}$ , and identifying a suitable value of  $b_{ii}$  while satisfying the system constraints and design objective. It can be accomplished by forming a functional optimization problem. Also, the design specifications are comprehensively represented by a new objective function. In the optimization procedure, by changing the closed-loop step responses according to its automatically selected controller parameters and calculating the objective function value at every generation, the iterative algorithm searches the optimal parameters for the controller subjected to the design specifications.

In the tuning of the controller, the objective function can be formed by different performance index that considers the step responses of the entire system. Typical performance index in the time domain includes integral square error (ISE), integral of absolute error (IAE), integral time absolute error (ITAE) [33], rise time ( $T_r$ ), settling time ( $T_s$ ), overshoot (OS), and steady-state error ( $E_{ss}$ ). The selection of these factors and form of the function can be determined depending on the design requirements. In this work, the desired control performance should have a small or no overshoot in the step response with a minimal settling time, and the control signal should be smooth within the physical limit. Hence, we defined the objective function  $F$  in this work as a linear combination of the ISE, integral of the square of the control signal, the overshoot OS, and the one percent settling time  $T_s$  [34]:

$$F = \sum_{i=1}^3 \alpha \int (y_i - r)^2 + \beta \int u_i^2 + \sigma (OS_i) + \varepsilon (T_{s,i}) \quad (20)$$

where the variables of  $\alpha$ ,  $\beta$ ,  $\sigma$ , and  $\varepsilon$  are the adjustment parameters. The values of these parameters are generally selected by using trial-and-error method. During the minimization of the objective function, all of the performance indexes are minimized and all of the disadvantaged controller parameters caused to system unstable or a poor performance will be eliminated by the algorithm.

Using the proposed objective function (20), the parameter tuning for the controller becomes a function optimization problem. This method combines a variety of performance indices which can be selected and weighted as required. Then the desired control performance and its parameter setting

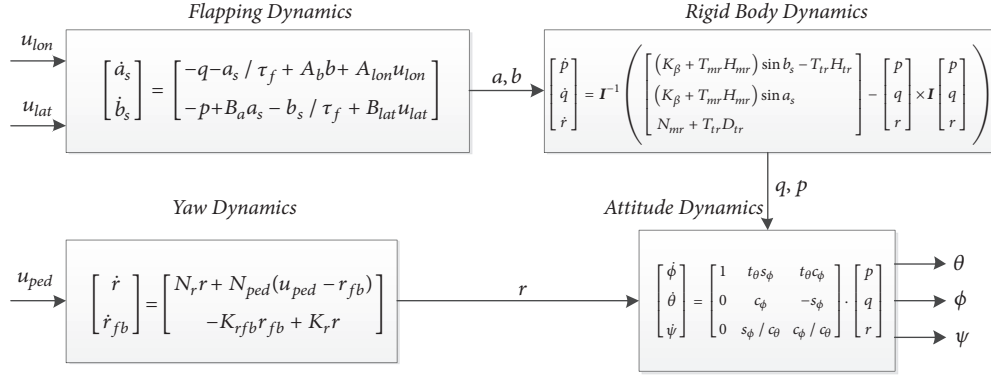


FIGURE 4: Interconnection of the helicopter dynamics model. The terms associated with the gravity force are disregarded.

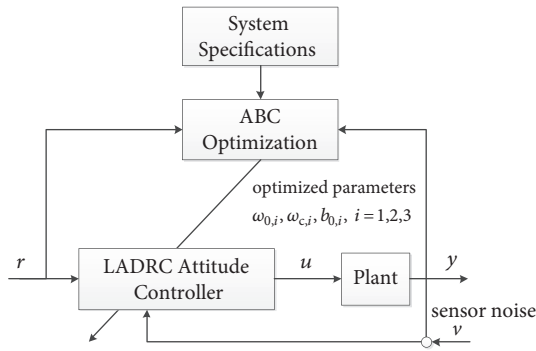


FIGURE 5: LADRC tuning scheme with ABC.

can be found by minimizing the value of (20). It makes this method different to the traditional optimal control method. Since (20) is nonlinear and discontinuous, simple search methods are usually lost in local optimum, as shown in [35]. Advanced search methods like GA, PSO, and ABC provide us with efficient solutions for solving this problem.

**4.2. ABC Algorithm.** In order to introduce the search mechanism of ABC algorithm, we should define three essential components: employed bees, unemployed bees, and food source [36]. And the unemployed bees are divided into the following bees and scout bees. The population of the colony bees is  $N_s$ , the number of employed bees is  $N_e$ , and the number of unemployed bees is  $N_u$ , which satisfies the relation  $N_s = 2N_e = 2N_u$ . We also define  $D$  as the dimension of solution vector, i.e., the number of the unknown parameters. ABC algorithm treats each solution vector as a food source and combines the global search of unemployed with the local search of employed bees. The detailed procedure of executing the proposed algorithm is described as follows.

**Step 1.** Randomly initialize a set of possible solutions  $(x_1, \dots, x_{N_s})$ , and the particular solution  $x_i$  can be governed by

$$x_i^j = x_{\min}^j + \text{rand}(0, 1) (x_{\max}^j - x_{\min}^j) \quad (21)$$

where  $j \in \{1, \dots, D\}$  denotes the  $j$ th dimension of the solution vector.  $x_{\min}^j$  and  $x_{\max}^j$  mean the lower and upper bounds, respectively.

**Step 2.** Apply a specific function to calculate the fitness of the solution  $x_i$  according to the following equations and select the top  $N_e$  best solutions as the number of the employed bees:

$$fit_i = \frac{1}{(1 + F_i)} \quad (22)$$

where  $fit_i$  is the fitness function and  $F_i$  is objective function depicted in (20).

**Step 3.** Each employed bee searches new solution in the neighborhood of the current position vector in the  $n$ th iteration as follows:

$$v_i^j = x_i^j + \lambda_i^j (x_i^j - x_k^j) \quad (23)$$

where  $k \in \{1, \dots, D\}$ ,  $k \neq i$ , both  $k$  and  $j$  are randomly generated, and  $\lambda_i^j$  is a random parameter in the range from -1 to 1. In order to ensure that the algorithm evolves to the global optimal, we apply the greedy selection equation (22) to choose the better solution between  $v_i^j$  and  $x_i^j$  into the next generation:

$$x_i^j = \begin{cases} v_i^j, & fit(v_i^j) > fit(x_i^j) \\ x_i^j, & fit(v_i^j) \leq fit(x_i^j) \end{cases} \quad (24)$$

**Step 4.** Each following bee selects an employed bee to trace according to the parameter of probability value. The formula of the probability method is described as

$$P_i = \frac{fit_i}{\sum_{i=1}^{N_e} fit_i} \quad (25)$$

**Step 5.** The following bee searches in the neighborhood of the selected employed bee's position to find new solutions. Update the current solution according to their fitness.

**Step 6.** If the search time *trial* is larger than the pre-determined threshold *limit* and the optimal value cannot

TABLE 2: Tuning performance of trial-and-error method, GA, PSO, and ABC algorithm.

Applied process	Time domain performance				
	$T_r/s$	OS/%	$T_s/s$	$E_{ss}/rad$	$F$
trial-and-error	0.70	2.33	1.17	0	1.2351
	0.55	1.30	0.77	0	
	0.37	1.86	0.65	0	
GA	0.596	2.13	0.97	0	1.013
	0.514	1.74	0.80	0	
	0.303	1.27	0.48	0	
PSO	0.62	2.01	0.94	0	0.9713
	0.53	1.82	0.81	0	
	0.30	1.11	0.40	0	
ABC	0.60	2.08	0.96	0	0.9315
	0.57	1.60	0.86	0	
	0.35	0.72	0.31	0	

be improved, the location vector can then be reinitialized randomly by scout bees according to the following equation:

$$x_i(n+1) = \begin{cases} x_{\min} + \text{rand}(0, 1)(x_{\max} - x_{\min}), & \text{trial} > \text{limit} \\ x_i(n), & \text{trial} \leq \text{limit} \end{cases} \quad (26)$$

*Step 7.* Output the best solution parameters achieved at the present time, and go back to Step 3 until termination criteria  $T_{\max}$  are met.

## 5. Simulation Tests

For best performance of optimization, we compare the results of ABC with the existing search iterative algorithm methods, including the trial-and-error method, GA, and PSO. We set the population size as 20 and iteration numbers as 50 for each algorithm. The adjustment parameters ( $\alpha$ ,  $\beta$ ,  $\sigma$ ,  $\varepsilon$ ) are selected as 1, 1, 0.1, and 0.2, respectively. The step command with the value of 0.2618 rad is applied to each of the input channels. 0.1% measurement white noise is added to the plant. For GA, the crossover probability and mutation probability are chosen as 0.8 and 0.2, respectively. For PSO, the optimal parameters, i.e., social, individual and inertia weight, are set to 2, 2, and 0.8, respectively. Finally, for ABC the threshold is set to  $\text{limit} = 5$ . The results are presented in Table 2 and Figure 8.

Figure 6 shows the evolution curves of ABC, GA, and PSO. The figure demonstrates that the objective function reduces as the generation iterates with time, gradually converging to an optimal result. Compared with GA and PSO, ABC achieves a better result with smaller objective function after 28 iterations. Table 2 indicates that all of the controllers have no steady-state error and that the trial-and-error method gets the largest time domain index. The ABC-optimized LADRC responds to the input and stabilizes the system faster than other three methods. In summary, the results suggest that our proposed method outperforms

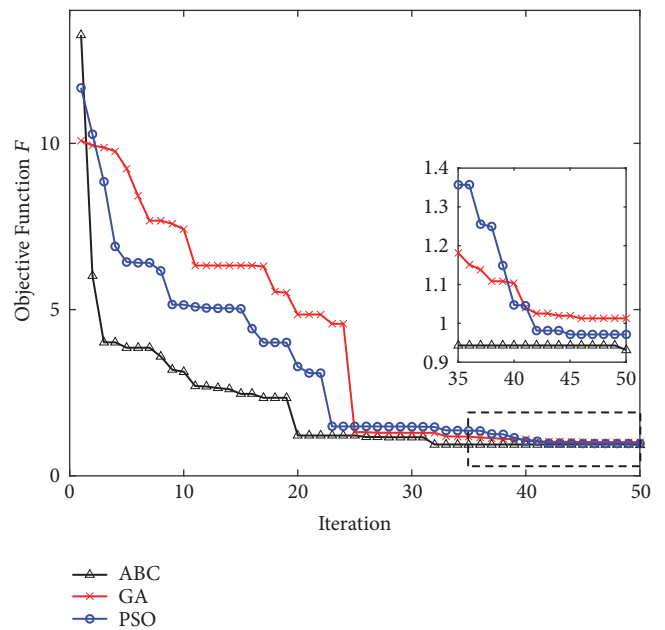


FIGURE 6: Evolutionary curves of the three algorithms.

other techniques in terms of rising time, settling time, and quadratic performance index.

To assess the improvements of the proposed controller, the closed-loop performance of helicopter attitude control with ABC-based LADRC and LQG is compared and analyzed by attitude tracking test under wind disturbance. The LQG controller is designed based on the linear model of Trex-600 helicopter; it is also implemented experimentally in [13]. As shown in Figure 7, the LQG controller consists of a state estimator based on Kalman filter and a MIMO state-feedback controller, which ensures that the output  $\Theta$  tracks the reference command  $r$  and rejects process disturbances and measured output noise. The Kalman filter produces estimates  $\hat{x}$  of the plant. The observer gain  $L_f$  and optimal state feedback gain  $K_f$  are achieved by solving two independent Riccati equations [14]

TABLE 3: Parameters of LADRC and LQG.

Results	Controllers	
	LADRC	LQG
Optimal parameters	$w_{0,1} = 126.50$	$\mathbf{Q} = \text{diag}(0, \dots, 0, 79.11, 242.98, 72.78)$ $\mathbf{R} = \text{diag}(1, 1, 1)$ $\mathbf{Q}_f = \text{diag}([0.01, 0.01, 0.01]);$ $\mathbf{R}_f = \text{diag}([0.01, 0.01, 0.01]);$
	$w_{c,1} = 11.81$	
	$b_{01} = 658.66$	
	$w_{0,2} = 116.67$	
	$w_{c,2} = 12.40$	
	$b_{02} = 638.15$	
	$w_{0,3} = 160.45$	
	$w_{c,3} = 19.32$	
	$b_{03} = -163.33$	
$F$	1.1355	1.7086

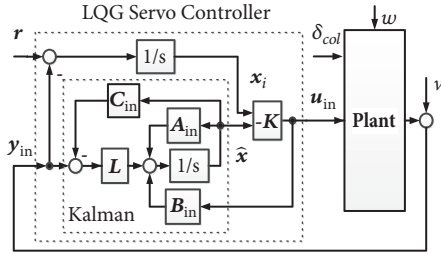


FIGURE 7: LQG controller.

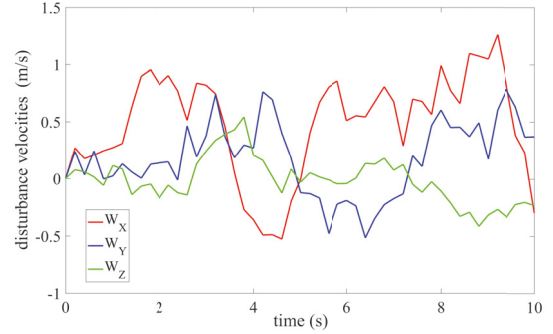


FIGURE 8: Wind disturbance vector.

$$\mathbf{K}_f = \mathbf{R}^{-1} \bar{\mathbf{B}}^T \mathbf{P} \quad (27)$$

$$\bar{\mathbf{A}}^T \mathbf{P} + \mathbf{P} \bar{\mathbf{A}} - \bar{\mathbf{P}} \bar{\mathbf{B}} \mathbf{R}^{-1} \bar{\mathbf{B}}^T \mathbf{P} + \mathbf{Q} = \mathbf{0}$$

$$\mathbf{L}_f = \mathbf{P}_f \mathbf{C}_{in}^T \mathbf{R}_f^{-1} \quad (28)$$

$$\mathbf{P}_f \mathbf{A}_{in}^T + \mathbf{A}_{in} \mathbf{P}_f - \mathbf{P}_f \mathbf{C}_{in}^T \mathbf{R}_f^{-1} \mathbf{C}_{in} \mathbf{P}_f + \mathbf{G} \mathbf{Q}_f \mathbf{G}^T = \mathbf{0}$$

where  $\mathbf{Q}$  and  $\mathbf{R}$  are symmetric weight matrices;  $\mathbf{Q}_f$  and  $\mathbf{R}_f$  are covariance matrices of process disturbances  $w$  and measured output noise  $v$ , respectively. It is obvious that the choice of weighting matrices ( $\mathbf{Q}, \mathbf{R}$ ) dominates the closed-loop performance.

Using the proposed method to optimize LQG, Table 3 summarizes the optimal parameters and objective values of these two controllers. It is observed that objective value of LQG is 1.5 times larger than that of LADRC. Hence, LADRC achieves better performance than LQG.

To simulate the measurement noise of the helicopter, the white noise is included in the output of the plant. The wind turbulence disturbances ( $W_X, W_Y, W_Z$ ), as shown in Figure 8, are also injected to the velocity vector  $\mathbf{V}$  along body frame  $X_B$ -,  $Y_B$ -, and  $Z_B$ -axes. Here, a shaping filter [37]

modeled by independently exciting of the correlated Gauss-Markov processes is chosen for the wind components:

$$\begin{bmatrix} \dot{W}_X \\ \dot{W}_Y \\ \dot{W}_Z \end{bmatrix} = \begin{bmatrix} -\frac{1}{\tau_s} & 0 & 0 \\ 0 & -\frac{1}{\tau_s} & 0 \\ 0 & 0 & -\frac{1}{\tau_s} \end{bmatrix} \begin{bmatrix} W_X \\ W_Y \\ W_Z \end{bmatrix} + \rho \mathbf{B}_W \begin{bmatrix} d_X \\ d_Y \\ d_Z \end{bmatrix} \quad (29)$$

where  $\tau_s$  is the correlation time of the wind;  $\rho$  is the scalar weighting factor;  $\mathbf{B}_W$  is the turbulence input identity matrix;  $d_X, d_Y$ , and  $d_Z$  are independent with zero mean.

Figures 9 and 10 show the roll and pitch responses and tracking error of the two control systems. We can observe that LADRC controller has more advanced performance in attitude tracking and disturbance resisting as compared to its counterpart. Figure 11 shows that LADRC controller responds faster and has smaller interfere between channels. For the LQG controller, however, the oscillation of  $u_{lon}$  increases apparently when there is a change in  $u_{lat}$ . Figures 12 and 13 show the angular velocities versus their estimates of both controllers. LESO has more effective estimation performance than Kalman filter, which means faster compensating for the

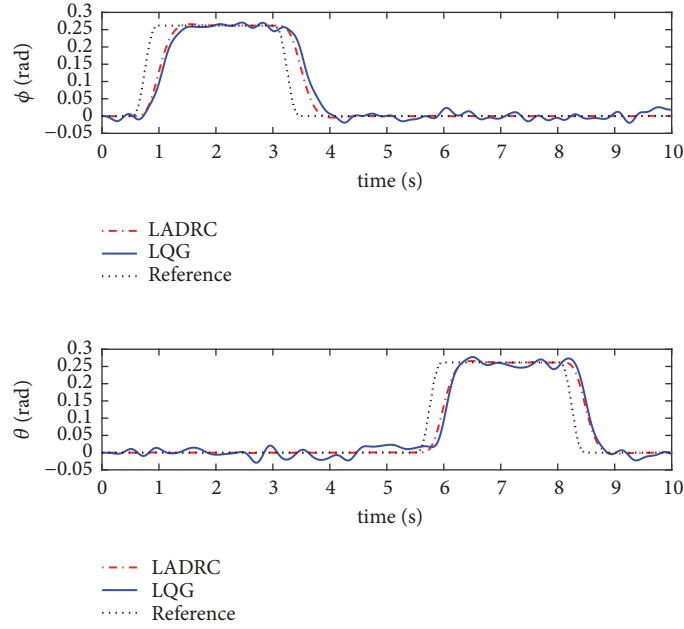


FIGURE 9: Attitude responses of both controllers with wind disturbance.

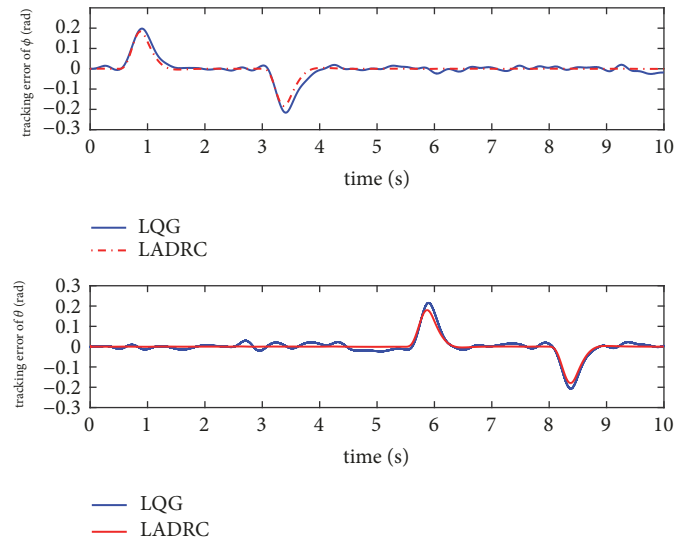


FIGURE 10: Tracking error of both controllers.

coupling effects and disturbances. All the simulation results indicate that the proposed ABC-optimized LADRC is the perfect control optimization strategy in terms of both the control performance and efficiency of design and parameter tuning. It obtains the lowest objective value and fastest convergence speed. But above all, LQG relies on the precise linear model of the plant, while LADRC only needs the input gains  $b_{ii}$  that can be even considered as the tuning parameter.

## 6. Conclusion

In this paper, the ABC algorithm is first applied to tune the controller parameters of LADRC-based DDC controller for a small-scale unmanned helicopter. With the proposed

method, the decoupling control of small helicopters is reformulated as a disturbance rejection one, with only the orders of each input-output pairs of the system. The controller optimization is formulated as a function optimization problem and an objective function is proposed for multiple conflicting performance specifications. Four different optimization algorithms are investigated and evaluated in the search of global optimum. The proposed controller is also compared with the traditional LQG technique on the performance of state estimation and disturbance rejection. The simulation results verify the robustness and effectiveness of the ABC-optimized DDC strategic. As future works, the presented strategic will be utilized to design a path following controller for our helicopter and test its reliability in real flight experiments.

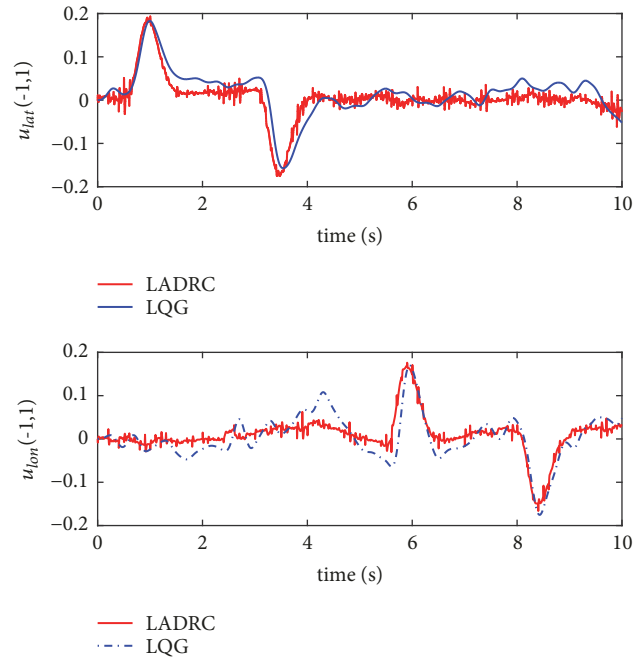


FIGURE 11: Control signals of both controllers.

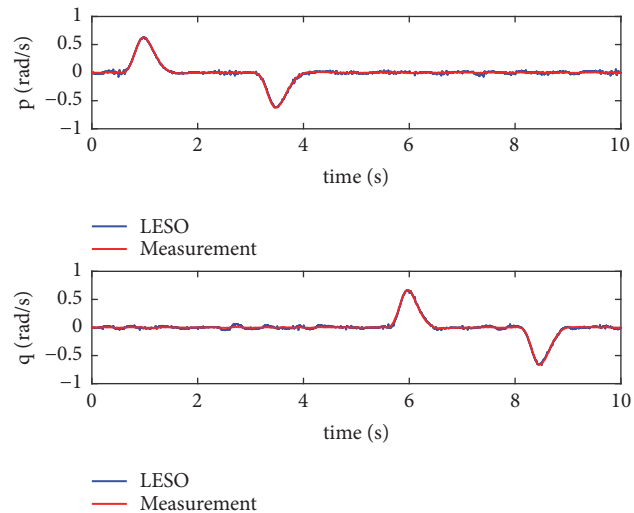


FIGURE 12: Performance of the LESO.

## Acronyms

ABC: Artificial bee colony  
 ADRC: Active disturbance rejection control  
 BF: Body frame  
 CG: Center of gravity  
 DDC: Dynamic decoupling control  
 ESO: Extended state observer  
 GA: Genetic algorithm  
 IAE: Integral of absolute error  
 ISE: Integral square error  
 ITAE: Integral time absolute error

LADRC: Linear active disturbance rejection control  
 LESO: Linear extended state observer  
 LQG: Linear quadratic Gaussian  
 LQI: Linear quadratic integral  
 LQR: Linear quadratic regulator  
 MIMO: Multi-input multi-output  
 PD: Proportional derivative  
 PID: Proportional integral derivative  
 PSO: Particle swarm optimization  
 SISO: Single-input/single-output  
 UAVs: Unmanned aerial vehicles.

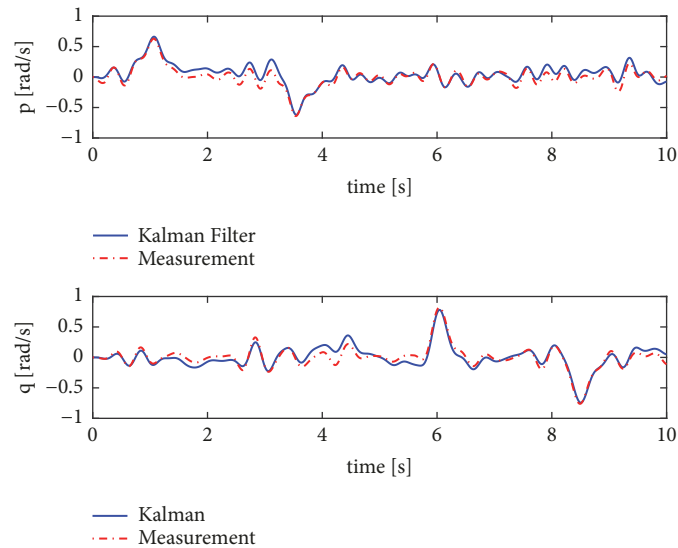


FIGURE 13: Performance of the Kalman filter.

## Data Availability

The data used to support the findings of this study are available from the corresponding author upon request.

## Conflicts of Interest

The authors declare that they have no conflicts of interest.

## Acknowledgments

This work was partially supported by the Foundation Research Project of Jiangsu Province (the Natural Science Fund no. K20170315) and Changzhou Sci&Tech Program of China (Grant no. CJ20179017).

## References

- [1] H. Xie and A. F. Lynch, "State transformation-based dynamic visual servoing for an unmanned aerial vehicle," *International Journal of Control*, vol. 89, no. 5, pp. 892–908, 2016.
- [2] L. Huang, H. Qu, P. Ji, X. Liu, and Z. Fan, "A novel coordinated path planning method using k-degree smoothing for multi-UAVs," *Applied Soft Computing*, vol. 48, pp. 182–192, 2016.
- [3] J. Zhou, L. R. Khot, T. Peters, M. D. Whiting, Q. Zhang, and D. Granatstein, "Efficacy of unmanned helicopter in rainwater removal from cherry canopies," *Computers and Electronics in Agriculture*, vol. 124, pp. 161–167, 2016.
- [4] C. Goerzen, Z. Kong, and B. Mettler, "A Survey of Motion Planning Algorithms from the Perspective of Autonomous UAV Guidance," *Journal of Intelligent & Robotic Systems*, vol. 57, no. 1–4, pp. 65–100, 2010.
- [5] H. Shim, T. Koo, F. Hoffmann, and S. Sastry, "A comprehensive study of control design for an autonomous helicopter," in *Proceedings of the 37th IEEE Conference on Decision and Control*, pp. 3653–3658, Tampa, FL, USA.
- [6] B. Mettler, *Identification Modeling and Characteristics of Miniature Rotorcraft*, Springer Science & Business Media, New York, NY, USA, 2013.
- [7] H. J. Kim and D. H. Shim, "A flight control system for aerial robots: algorithms and experiments," *Control Engineering Practice*, vol. 11, no. 12, pp. 1389–1400, 2003.
- [8] M. Vijaya Kumar, S. Suresh, S. N. Omkar, R. Ganguli, and P. Sampath, "A direct adaptive neural command controller design for an unstable helicopter," *Engineering Applications of Artificial Intelligence*, vol. 22, no. 2, pp. 181–191, 2009.
- [9] C.-T. Lee and C.-C. Tsai, "Adaptive backstepping integral control of a small-scale helicopter for airdrop missions," *Asian Journal of Control*, vol. 12, no. 4, pp. 531–541, 2010.
- [10] H. Voos, "Nonlinear control of a quadrotor micro-uav using feedback-linearization," in *Proceedings of the IEEE International Conference on Mechatronics (ICM '09)*, pp. 1–6, IEEE, April 2009.
- [11] S. Ahrens, D. Levine, G. Andrews, and J. How, "Vision-based guidance and control of a hovering vehicle in unknown, GPS-denied environments," in *Proceedings of the 2009 IEEE International Conference on Robotics and Automation (ICRA)*, pp. 2643–2648, Kobe, May 2009.
- [12] B. Kadmiry, P. Bergsten, and D. Driankov, "Autonomous helicopter control using fuzzy gain scheduling," in *Proceedings of the 2001 ICRA. IEEE International Conference on Robotics and Automation*, pp. 2980–2985, Seoul, South Korea.
- [13] R. Enns and J. Si, "Helicopter trimming and tracking control using direct neural dynamic programming," *IEEE Transactions on Neural Networks and Learning Systems*, vol. 14, no. 4, pp. 929–939, 2003.
- [14] J. Shin, K. Nonami, and D. Fujiwara, "Model-based optimal attitude and positioning control of small-scale unmanned helicopter," *Robotica*, vol. 23, no. 1, pp. 51–63, 2005.
- [15] A. Budiyo and S. S. Wibowo, "Optimal Tracking Controller Design for a Small Scale Helicopter," *Journal of Bionic Engineering*, vol. 4, no. 4, pp. 271–280, 2007.
- [16] J. Gadewadikar, F. L. Lewis, K. Subbarao, K. Peng, and B. M. Chen, "H-infinity static output-feedback control for rotorcraft"

- Journal of Intelligent & Robotic Systems*, vol. 54, no. 4, pp. 629–646, 2009.
- [17] G. Cai, B. Wang, B. M. Chen, and T. H. Lee, “Design and implementation of a flight control system for an unmanned rotorcraft using RPT control approach,” *Asian Journal of Control*, vol. 15, no. 1, pp. 95–119, 2013.
- [18] Q. Zheng, Z. Chen, and Z. Gao, “A practical approach to disturbance decoupling control,” *Control Engineering Practice*, vol. 17, no. 9, pp. 1016–1025, 2009.
- [19] J. Han, “Nonlinear design methods for control systems,” *IFAC Proceedings Volumes*, vol. 32, no. 2, pp. 1531–1536, 1999.
- [20] Z. Gao, Y. Huang, and J. Han, “An alternative paradigm for control system design,” in *Proceedings of the 40th IEEE Conference on Decision and Control (CDC '01)*, vol. 5, pp. 4578–4585, Orlando, Fla, USA, December 2001.
- [21] . Yi Huang, . Kekang Xu, . Jingqing Han, and J. Lam, “Flight control design using extended state observer and non-smooth feedback,” in *Proceedings of the 40th Conference on Decision and Control*, pp. 223–228, Orlando, FL, USA.
- [22] Q. Zheng, Z. Chen, and Z. Gao, “A Dynamic Decoupling Control Approach and Its Applications to Chemical Processes,” in *Proceedings of the 2007 American Control Conference*, pp. 5176–5181, New York, NY, USA, July 2007.
- [23] Q. Zheng and Z. Gao, “Motion control design optimization: Problem and solutions,” *Int. J. Intell. Control Syst*, vol. 10, pp. 269–276, 2005.
- [24] D. Karaboga, “An idea based on honey bee swarm for numerical optimization,” 2005.
- [25] M. Abachizadeh, M. R. Yazdi, and A. Yousefi-Koma, “Optimal tuning of PID controllers using Artificial Bee Colony algorithm,” in *Proceedings of the 2010 IEEE/ASME International Conference on Advanced Intelligent Mechatronics (AIM)*, pp. 379–384, Montreal, QC, Canada, July 2010.
- [26] C. Sun and D. Haibin, “Artificial bee colony optimized controller for unmanned rotorcraft pendulum,” *Aircraft Engineering and Aerospace Technology*, vol. 85, no. 2, pp. 104–114, 2013.
- [27] O. Abedinia, B. Wyns, and A. Ghasemi, “Robust fuzzy PSS design using ABC,” in *Proceedings of the 2011 10th International Conference on Environment and Electrical Engineering (EEEIC)*, pp. 1–4, Rome, Italy, May 2011.
- [28] L. Ding, H. T. Wu, and Y. Yao, “Chaotic artificial bee colony algorithm for system identification of a small-scale unmanned helicopter,” *International Journal of Aerospace Engineering*, vol. 2015, Article ID 801874, 11 pages, 2015.
- [29] V. Gavrillets, B. Mettler, and E. Feron, “Nonlinear model for a small-size acrobatic helicopter,” in *Proceedings of the AIAA Guidance, Navigation, and Control Conference and Exhibit*, pp. 6–9, August 2001.
- [30] B. Mettler and T. Kanade, “System Identification Modeling of a Model-Scale Helicopter,” *Robotics*, vol. 1, p. pp, 2000, <http://citeseerx.ist.psu.edu/viewdoc/download>.
- [31] Z. Gao, “Scaling and bandwidth-parameterization based controller tuning,” in *Proceedings of the American Control Conference*, pp. 4989–4996, Denver, Colo, USA, June 2003.
- [32] Z. Gao, “Active disturbance rejection control: a paradigm shift in feedback control system design,” in *Proceedings of the American Control Conference (ACC '06)*, p. 7, IEEE, Minneapolis, Minn, USA, June 2006.
- [33] L. dos Santos Coelho, “Tuning of PID controller for an automatic regulator voltage system using chaotic optimization approach,” *Chaos, Solitons & Fractals*, vol. 39, no. 4, pp. 1504–1514, 2009.
- [34] A. Bagis, “Determination of the PID controller parameters by modified genetic algorithm for improved performance,” *Journal of Information Science and Engineering*, vol. 23, no. 5, pp. 1469–1480, 2007.
- [35] F. J. Goforth, “On motion control design and tuning techniques,” in *Proceedings of the 2004 American Control Conference (AAC)*, pp. 716–721, Boston, MA, USA, July 2004.
- [36] D. Karaboga and B. Basturk, “A powerful and efficient algorithm for numerical function optimization: artificial bee colony (ABC) algorithm,” *Journal of Global Optimization*, vol. 39, no. 3, pp. 459–471, 2007.
- [37] W. E. Hall and A. E. Bryson, “Inclusion of rotor dynamics in controller design for helicopters,” *Journal of Aircraft*, vol. 10, no. 4, pp. 200–206, 1973.

